Inorg. Chem. **1994**, *33*, 6007–6011 **6007**

Crystal Structure and Magnetic Properties of $[\{Ni_2(dpt)_2(\mu\text{-}ox)(\mu\text{-}N_3)\}_n](PF_6)_n$: A New Strategy To Obtain $S = 1$ Alternating Chains

Albert Escuer,[*,†] **Ramon Vicente,**[†] **Xavier Solans,**[‡] **and Mercé Font-Bardía**[‡]

Department de Química Inorgànica, Universitat de Barcelona, Diagonal 647, 08028-Barcelona, Spain, and Departament de Cristal.lografia i Mineralogia, Universitat de Barcelona, Martí Franqués s/n, 08028-Barcelona, Spain

Received May 18, 1994[®]

A new alternating magnetic chain with local spin S = 1, with formula $[\{Ni_2(dpt)_2(\mu\text{-}ox)(\mu\text{-}N_3)\}_n](PF_6)_n$, in which dpt is the triamine bis-(3-aminopropyl)amine, was synthesized and structurally characterized. The title compound $[C_{14}H_{34}N_9Ni_2O_4]_n{\cdot}nPF_6$ crystallizes in the monoclinic system, space group $P2_1/a$, with fw = 654.87, $a = 10.989(1)$ Å, $b = 19.357(2)$ Å $c = 12.598(2)$ Å, $\beta = 107.27(1)°$, $Z = 4$, $R = 0.033$, and $R_w = 0.033$. Structurally $[\{Ni_2(dpt)_2(\mu\text{-}ox)(\mu\text{-}N_3)\}_n](PF_6)_n$ can be described as formed by $[Ni(dpt)]^{2+}$ units linked, alternately, by one oxalato and one azido bridge. A similar compound formuled as $[\{Ni_2(Medpt)_2(\mu\text{-}ox)(\mu\text{-}N_3)\}_n](ClO_4)_n$ where Medpt is the triamine methylbis(3-aminopropyl)amine was also synthesized. The susceptibility measurement between 300 and 4 K of $[\{Ni_2(dpt)_2(\mu\text{-}ox)(\mu\text{-}N_3)\}_n](PF_6)_n$ indicates an antiferromagnetic behavior with $J = -27.4$ cm^{-1}, $J' = \alpha J = -2.7$ cm^{-1}, alternating parameter $\alpha = 0.1$, $g = 2.19$.

Introduction

Monodimensional alternating magnetic systems in which the local spins are $S = {}^1/_2$ are well-known, and experimental examples have been exhaustively studied from the magnetic point of view.[1] In contrast, this kind of system is practically unexplored when the local spin is greater than ${}^1/_2$ and bibliographic data indicate that only one $S = 1$ alternating system has been structurally and magnetically characterized[2] by Hatfield et al.: an alternating oxo-bridged chain of iron(IV), with an alternating parameter $\alpha = 0.40$. Following our work on polynuclear nickel(II)−pseudohalide systems,[3-10] we have recently characterized several $S = 1$ alternating systems[4,8-10] in which the bridging ligand is always the azido group coordinated in end-to-end fashion. These alternating systems can be structurally classified into two main groups: those in which the same bridge is repeated along the chain, but which present, in an alternating fashion, different bond parameters that are of sufficient importance to induce an alternation in the magnetic properties[8-10] (Figure 1A), and chains in which the magnetic alternating properties are derived from the different number of bridges of the same ligand arranged in alternating fashion,[4] (Figure 1B).

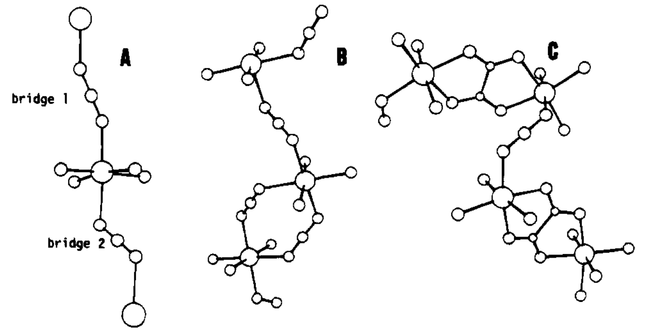

Figure 1. The three types of alternating $S = 1$ chains synthesized to date: (A) alternating bond parameters with the same bridging ligand; (B) alternating number of the same bridging ligands; (C) alternating ligands.

The aim of this work was to obtain the most obvious kind of alternating system, which would be possible if two different bridging ligands are placed alternately along the chain (Figure 1C). Thus we chosed as a starting point the dinuclear complexes $(\mu\text{-}ox)[Ni_2(L)_2(H_2O)_2](ClO_4)_2$, in which L is the tridentate ligand bis(3-aminopropyl)amine (dpt) or bis(3-aminopropyl)methylamine, (Medpt), structurally characterized by the authors,[11] in which each nickel atom is coordinated to one tridentate amine, one bridging oxalato group and one water molecule. The water molecule can act as a labile ligand in the presence of azide anion, which can link the $[(L)Ni{-}ox{-}Ni(L)]^{2+}$ structural units to generate an alternating monodimensional system. Using this strategy, two compounds formulated as $[\{Ni_2(Medpt)_2(\mu\text{-}ox)(\mu\text{-}N_3)\}_n](ClO_4)_n$ (**1**) and $[\{Ni_2(dpt)_2(\mu\text{-}ox)(\mu\text{-}N_3)\}_n](PF_6)_n$ (**2**) were obtained and the X-ray determination of the structure was performed for **2**.

The fit of the susceptibility data of regular alternating systems with an alternation in the J coupling parameter involves the use of analytical equations based in the Hamiltonian $H = -J\sum[S_{i-1}{\cdot}S_i + \alpha S_i{\cdot}S_{i+1}]$, where α is the alternating parameter, for which 0

[†] Department de Química Inorgànica.

[‡] Departament de Cristal.lografia i Mineralogia.

[®] Abstract published in *Advance ACS Abstracts*, November 15, 1994.

(1) Kahn, O. *Molecular Magnetism*; VCH Publishers: Weinheim, Germany, 1993; Chapter 11 and references therein.

(2) Hiller, W.; Strähle, J.; Datz, A.; Hanack, M.; Hatfield, W. E.; Haar, L. W.; Gütlich, P. *J. Am. Chem. Soc.* **1984**, *106*, 329.

(3) Escuer, A.; Vicente, R.; Ribas, J. *J. Magn. Magn. Mater.* **1992**, *110*, 181.

(4) Vicente, R.; Escuer, A.; Ribas, J.; Solans, X. *Inorg. Chem.* **1992**, *31*, 1726.

(5) Escuer, A.; Vicente, R.; Ribas, J.; El Fallah, M. S.; Solans, X. *Inorg. Chem.* **1993**, *32*, 1033.

(6) Vicente, R.; Escuer, A.; Ribas, J.; El Fallah, M. S.; Solans, X.; Font-Bardia, M. *Inorg. Chem.* **1993**, *32*, 1920.

(7) Escuer, A.; Vicente, R.; Ribas, J. El Fallah, M. S.; Solans, X.; Font-Bardia, M. *Inorg. Chem.* **1993**, *32*, 3727.

(8) Escuer, A.; Vicente, R.; El Fallah, M. S.; Solans, X.; Font-Bardia, M. *Inorg. Chem.* **1994**, *33*, 1842.

(9) Vicente, R.; Escuer, A.; El Fallah, M. S.; Ribas, J.; Solans, X.; Font-Bardia, M. *Inorg. Chem.*, submitted for publication.

(10) Escuer, A.; Vicente, R.; El Fallah, M. S.; Ribas, J.; Solans, X.; Font-Bardia, M. *J. Chem. Soc., Dalton Trans.* **1993**, 2975.

(11) Escuer, A.; Vicente, R.; Ribas, J.; Jaud, J.; Raynaud, B. *Inorg. Chim. Acta* **1994**, *216*, 139 and references therein.

0020-1669/94/1333-6007$04.50/0

Table 1. Crystal Data for $[\{Ni_2(dpt)_2(\mu\text{-ox})(\mu\text{-}N_3)\}_n](PF_6)_n$

formula	$[C_{14}H_{34}N_9Ni_2O_4]_n(PF_6)_n$
a, Å	10.989(1)
b, Å	19.357(2)
c, Å	12.598(2)
β, deg	107.27(1)
V, Å^3	2559.0(9)
Z	4
fw	654.87
space group	$P2_1/a$
T, °C	25
λ(Mo Kα), Å	0.710 69
d_{calc}, g/cm^{-3}	1.699
μ(Mo Kα), cm^{-1}	16.19
R^a	0.033
$R_w^{\ b}$	0.033

^{a} $R = \sum||F_o| - |F_c||/\sum|F_o|$. ^{b} $R_w = \sum w||F_o| - |F_c||/\sum w|F_o|$.

$\leq \alpha \leq 1$ values are possible. For $\alpha = 0$ the magnetic behavior corresponds to isolated dimeric entities and for $\alpha = 1$ the magnetic behavior corresponds to an homogeneous chain, which can be analyzed with the Weng equation.[12] Recently, the theoretical aspects of an alternating $S = 1$ system have been solved,[13] and a full characterization of the title compounds from magnetic point of view has been possible. The discussion of the magnetic properties along the text has been performed from the structural data of compound **2**.

Experimental Section

Synthesis Caution! Perchlorate salts of metal complexes with azide and organic ligands are potentially explosive. Only a small amount of material should be prepared, and it should be handled with caution.

Compound 1. A solution of 2 mmol of nickel(II) perchlorate hexahydrate in 30 mL of water was mixed with 2 mmol of Medpt ligand and 1 mmol of sodium oxalate. After 5 min of stirring, the resulting blue solution was mixed with 1 mmol of sodium azide dissolved in 10 mL of water. Slow evaporation of the resulting blue solution gave blue crystalline plates of the corresponding 1D compound. All the attempts to obtain good quality X-ray crystals were unsuccessful due to its tendency to form aggregates of small crystallyne plates. Compound **2** was obtained as for **1** starting from nickel(II) nitrate hexahydrate and adding to the resulting solution 2 mmol of potassium hexafluorophosphate. Slow evaporation of the resulting solution gave blue crystals of **2**.

Both complexes are soluble in water and insoluble in the common organic solvents. Anal. Calcd for **1**, $C_{16}H_{40}ClN_9Ni_2O_9$: C, 29.32; H, 6.15; N, 19.23; Cl, 5.41. Found: C, 29.5; H, 6.10; N, 19.6; Cl, 5.5. Anal. Calcd for 2, $C_{14}H_{34}F_6N_9Ni_2O_4P$: C, 25.67; H, 5.23; N, 19.25. Found: C, 25.6; H, 5.2; N, 19.2.

It is interesting to point out that the analogous reactions with L = Medpt and dpt using hexafluorophosphate and perchlorate counteranions, respectively, do not yield the 1D compounds and the corresponding dimeric μ-oxalato complexes were obtained instead.

Physical Measurements. Infrared spectra (4000−200 cm^{-1}) were recorded from KBr pellets in a Perkin-Elmer 1330 IR spectrophotometer. Magnetic measurements were carried out on microcrystalline powder with a pendulum type magnetometer (MANICS DSM8) equipped with a helium continuous-flow cryostat working in the temperature range 300−4 K, and a Brucker B E15 electromagnet. The magnetic field was 15 000 G, approximately. Diamagnetic corrections were estimated from Pascal tables.

Crystal Data Collection and Refinement. A crystal (0.5 × 0.5 × 0.1 mm) of **2** was selected and mounted on a Enraf-Nonius CAD4 diffractometer. Crystallographic data, conditions retained for the intensity data collection, and some features of the structure refinement are listed in Table 1. Accurate unit-cell parameters were determined from automatic centering of 25 reflections ($12 \leq \theta \leq 21°$) and refined by least-squares method. Intensities were collected with graphite-monochromatized Mo Kα radiation, using the $\omega-2\theta$ scan technique.

Table 2. Positional Parameters and Equivalent Isotropic Thermal Parameters (Å^2) and their Estimated Standard Deviations for $[\{Ni_2(dpt)_2(\mu\text{-ox})(\mu\text{-}N_3)\}_n](PF_6)_n$

atom	x/a	y/b	z/c	B_{eq}
Ni(1)	0.04104(2)	0.10904(1)	0.15049(2)	2.35(1)
Ni(2)	−0.43746(2)	0.18068(1)	−0.09358(2)	2.25(1)
O(1)	−0.08039(11)	0.19561(6)	0.12483(9)	2.60(4)
O(2)	−0.31920(11)	0.09326(6)	−0.04756(11)	2.86(4)
O(3)	−0.28051(10)	0.22422(6)	0.02871(10)	2.69(4)
O(4)	−0.13342(11)	0.06241(5)	0.07005(10)	2.80(4)
N(1)	−0.5340(1)	0.2772(1)	−0.1254(1)	3.01(5)
N(2)	−0.4894(1)	0.3256(1)	−0.0711(1)	2.75(5)
N(3)	0.0539(2)	0.1241(1)	−0.0197(1)	3.24(6)
N(4)	0.2036(2)	0.1681(1)	0.2118(1)	3.42(6)
N(5)	0.0136(2)	0.0966(1)	0.3074(1)	4.19(7)
N(6)	0.1260(2)	0.0137(1)	0.1482(2)	3.76(7)
N(7)	−0.3386(1)	0.2036(1)	−0.2087(1)	3.60(6)
N(8)	−0.5734(1)	0.1254(1)	−0.2165(1)	2.83(5)
N(9)	−0.5115(1)	0.1588(1)	0.0374(1)	3.10(6)
C(1)	−0.1913(1)	0.1821(1)	0.0632(1)	2.15(5)
C(2)	−0.2175(2)	0.1056(1)	0.0249(1)	2.36(5)
C(3)	0.1997(2)	0.2201(1)	0.2948(2)	4.28(8)
C(4)	0.1689(3)	0.1893(2)	0.3955(2)	5.28(11)
C(5)	0.0385(3)	0.1624(1)	0.3746(2)	4.99(11)
C(6)	0.0739(4)	0.0371(2)	0.3757(2)	6.25(14)
C(7)	0.0677(4)	−0.0290(1)	0.3126(3)	6.34(14)
C(8)	0.1656(3)	−0.0303(1)	0.2496(3)	5.81(13)
C(9)	−0.4096(2)	0.2213(2)	−0.3230(2)	4.78(10)
C(10)	−0.5076(3)	0.1667(2)	−0.3774(2)	5.28(11)
C(11)	−0.6110(2)	0.1569(2)	−0.3256(2)	4.76(9)
C(12)	−0.6878(2)	0.1043(1)	−0.1863(2)	3.60(7)
C(13)	−0.6526(2)	0.0683(1)	−0.0739(2)	4.37(9)
C(14)	−0.6263(3)	0.1162(1)	0.0230(2)	4.71(11)
P	0.6337(1)	0.0777(0)	0.3587(1)	6.75(4)
F(1)	0.5196(5)	0.1374(3)	0.2993(4)	2.34(3)
F(1)′	0.5374(5)	0.1339(3)	0.3451(4)	2.54(3)
F(2)	0.6843(3)	0.1038(2)	0.2614(2)	3.53(3)
F(3)	0.6901(6)	0.1267(3)	0.4503(5)	3.10(4)
F(3)′	0.7489(5)	0.1320(3)	0.4314(4)	2.67(3)
F(4)	0.5328(6)	0.0224(3)	0.2881(5)	2.88(4)
F(4)′	0.5568(6)	0.0315(3)	0.2568(5)	2.92(4)
F(5)	0.7721(4)	0.0289(2)	0.3786(3)	2.38(3)
F(5)′	0.7098(6)	0.0128(3)	0.3949(4)	3.01(4)
F(6)	0.5380(8)	0.0563(4)	0.4326(6)	4.02(6)
F(6)′	0.6241(6)	0.0502(3)	0.4709(4)	2.82(3)

^{a} $B_{eq} = 8\pi^2/3(\sum_i\sum_j U_{ij}a^*{}_j a_i a_j)$.

A total of 6843 reflections were measured in the range $2 \leq \theta \leq 30°$ and 5377 were assumed as observed, applying the condition $I \geq 2.5\sigma(I)$. R_{int} on $F = 0.023$. Three reflections were measured every 2 h as orientation and intensity control; significant intensity decay was not observed. Lorentz-polarization and absorption corrections[14] were made: $T_{min} = 0.74$; $T_{max} = 0.86$. The structure was solved by Patterson synthesis, using the SHELXS computer program,[15] and refined by the full-matrix least-squares method, with the SHELX76[16] computer program. The function minimized was $\sum w[[F_o] - [F_c]]^2$, where $w = (\sigma^2(F_o) + 0.0033\,[F_o]^2)^{-1}$; f, f', and f'' were taken from ref 17. Fluorine atoms of PF_6^- are disordered, (with the exception of F(2) for which the second position was not located), and an occupancy factor of 0.5 was assigned according to height of Fourier synthesis. Fluorine atoms were only refined isotropically. The position of all H atoms was computed and refined with an overall isotropic temperature factor using a riding model. The final R factor was 0.033 ($R_w = 0.033$). Number of parameters refined = 316. Maximum shift/esd = 0.2; maximum and minimum peaks in the final difference synthesis were 0.6 and −0.6 e Å^{-3}, respectively. Final atomic coordinates are given in Table 2.

---

(12) Weng, C. Y. Ph.D. Thesis, Carnegie Institute of Technology, 1968.

(13) Borras, J. J. Ph.D. Thesis, Universitat de València, Spain, 1991. Coronado, E.; et al. *Inorg. Chem.*, in press.

(14) DIFABS, Walker, N.; Stuart, D. *Acta Crystallogr.* **1983**, *A39*, 158.

(15) Sheldrick, G. M. *Acta Crystallogr.* **1990**, *A46*, 467.

(16) Sheldrick, G. M. SHELX. A computer program for crystal structure determination. University of Cambridge, England, 1976.

(17) *International Tables for X-ray Crystallography*, Kynoch Press: Birmingham, England, 1974; Vol. IV, pp 99−110 and 149.

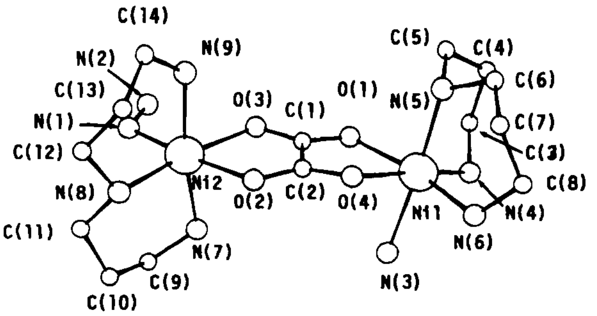

Figure 2. Labeled structure of $[\{Ni_2(dpt)_2(\mu\text{-}ox)(\mu\text{-}N_3)\}_n](PF_6)_n$ (2).

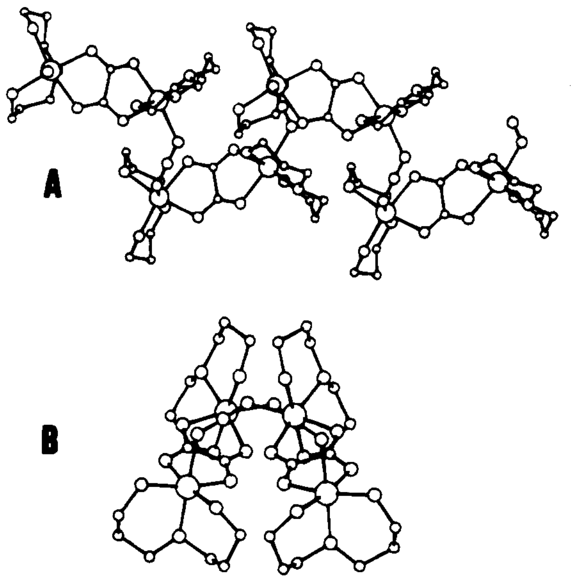

Figure 3. (A) View of the $[\{Ni_2(dpt)_2(\mu\text{-}ox)(\mu\text{-}N_3)\}_n](PF_6)_n$ chain (2) showing the alternate *fac* and *mer* coordination of the aminate ligand dpt. (B) Projection of 2 along the chain axis.

Results and Discussion

IR Spectra. The IR spectra of the two compounds are similar in the most important features: the two spectra show the characteristic bands of Medpt for **1** and dpt for **2**, a very strong absorption attributable to the azido ligand at 2050 cm^{-1}, an absorption centered at 1645 cm^{-1} (very strong, broad), attributable to the oxalato bridge and the bands due to the corresponding ClO_4^- (centered at 1100 cm^{-1}), and an absorption for the PF_6^- anion at 840 cm^{-1} for **1** and **2**, respectively.

Description of the Structure. The most interesting feature of the structure of $[\{Ni_2(dpt)_2(\mu\text{-}ox)(\mu\text{-}N_3)\}_n](PF_6)_n$ is that the compound can be defined as a chain in which each $Ni(dpt)^{2+}$ fragment is linked to the next unit by means of one oxalato and one azido bridge in a regular alternate fashion. Consequently, each nickel atom is coordinated to three nitrogen atoms of the aminate ligand, one nitrogen atom of an azido group and two oxygen atoms of the oxalato group, in an octahedral NiN_4O_2 environment. The atom-labeling scheme is shown in Figure 2. The oxalato group is coordinated in bis-bidentate form as occurs habitually, and the azido ligand is coordinated in the end-to-end mode. Two kinds of nonequivalent nickel atoms are present in the chain, which show different bond parameters with respect to the bridging ligands and different coordination modes of the aminate ligand: the amine is coordinated to Ni(1) in *fac* arrangement whereas the amine is coordinated to Ni(2) in *mer* arrangement as can be seen in Figure 3. The main bond distances and angles are shown in Table 3. The bond parameters of the bridges are comparable with those reported in the literature for Ni−Ni systems with oxalato or azido bridges, but certain features of this structure which can influence the magnetic behavior should be pointed out. As regards the azido bridge, the most remarkable facts are the asymmetric end-to-end coordination, Ni(1)−N(3) = 2.209(2) Å, Ni(2)−N(1) = 2.127(1) Å, Ni(1)−N(3)−N(2)′ = 120.4(1)° and Ni(2)−N(1)−N(2) = 119.4(1)°, and the unusually high value (102.1°) for the torsion angle determined by the mean planes Ni(1)′−N(3)′−N(2)−N(1) and N(3)′−N(2)−N(1)−Ni(2), (see Figure 4a). For the oxalato-bridged systems reported to date the fragment $M\text{-}C_2O_4\text{-}M$ is strictly planar, but in 2 a significant distortion from planarity due to packing requirements is found (Figure 4b and Table 4). The mean plane O(1)−O(4)−C(1)−C(2)−O(2)−O(3) (plane 1) contains the C-atoms whereas the oxygen atoms are out of this plane, showing a deviation of 0.091, 0.090, −0.084, and −0.087 Å for O(1), O(2), O(3), and O(4) respectively. When Ni(1) and Ni(2) are added to the previous plane (plane 2) the two nickel atoms are 0.197 Å for Ni(1) and 0.134 Å for Ni(2) out of the eight-atom mean plane. The dihedral angles between plane 1 and the planes determined for Ni(1)−O(1)−O(4)−N(4)−N(6) (plane 3) and Ni(2)−O(2)−O(3)−N(1)−N(8) (plane 4) are 16.3° and 6.5° respectively (Table 4). The dihedral angle between the planes 3 and 4 takes a value of 22.3° value.

Table 3. Selected Bond Distances (Å) and Angles (deg) for $[\{Ni_2(dpt)_2(\mu\text{-}ox)(\mu\text{-}N_3)\}_n](PF_6)_n$

	Distances		
	Nickel Environment		
Ni(1)−O(1)	2.106(1)	Ni(2)−O(2)	2.107(1)
Ni(1)−O(4)	2.089(1)	Ni(2)−O(3)	2.117(1)
Ni(1)−N(3)	2.209(2)	Ni(2)−N(1)	2.127(1)
Ni(1)−N(4)	2.068(2)	Ni(2)−N(7)	2.102(2)
Ni(1)−N(5)	2.100(2)	Ni(2)−N(8)	2.098(1)
Ni(1)−N(6)	2.072(2)	Ni(2)−N(9)	2.088(1)
Ni(1)−Ni(2)	5.425(1)	Ni(1)−Ni(2)′	5.149(1)
	Oxalato and Azido Groups		
C(1)−O(1)	1.263(2)	N(1)−N(2)	1.178(2)
C(1)−O(3)	1.249(2)	N(2)−N(3)	1.188(2)
C(2)−O(2)	1.238(2)		
C(2)−O(4)	1.252(2)		
C(1)−C(2)	1.557(2)		
	Angles		
	Nickel Environment		
O(4)−Ni(1)−O(1)	79.7	O(3)−Ni(2)−O(2)	79.4
N(3)−Ni(1)−O(1)	88.1(1)	N(1)−Ni(2)−O(2)	171.7
N(3)−Ni(1)−O(4)	84.3(1)	N(1)−Ni(2)−O(3)	92.3
N(4)−Ni(1)−O(1)	93.2(1)	N(7)−Ni(2)−O(2)	87.5(1)
N(4)−Ni(1)−O(4)	170.7(1)	N(7)−Ni(2)−O(3)	86.6(1)
N(4)−Ni(1)−N(3)	89.6(1)	N(7)−Ni(2)−N(1)	90.9(1)
N(5)−Ni(1)−O(1)	88.5(1)	N(8)−Ni(2)−O(2)	92.3(1)
N(5)−Ni(1)−O(4)	92.2(1)	N(8)−Ni(2)−O(3)	171.1(1)
N(5)−Ni(1)−N(3)	175.5(1)	N(8)−Ni(2)−N(1)	95.9(1)
N(5)−Ni(1)−N(4)	93.5(1)	N(8)−Ni(2)−N(7)	89.9(1)
N(6)−Ni(1)−O(1)	166.9(1)	N(9)−Ni(2)−O(2)	88.4(1)
N(6)−Ni(1)−O(4)	87.7(1)	N(9)−Ni(2)−O(3)	86.0(1)
N(6)−Ni(1)−N(3)	86.8(1)	N(9)−Ni(2)−N(1)	92.1(1)
N(6)−Ni(1)−N(4)	98.9(1)	N(9)−Ni(2)−N(7)	172.1(1)
N(6)−Ni(1)−N(5)	95.8(1)	N(9)−Ni(2)−N(8)	97.0(1)
Ni(1)−O(1)−C(1)	112.4(1)	Ni(2)−O(2)−C(2)	113.3(1)
Ni(1)−O(4)−C(2)	112.3(1)	Ni(2)−O(3)−C(1)	112.3(1)
Ni(1)−N(3)−N(2)′	120.4(1)	Ni(2)−N(1)−N(2)	119.4(1)
	Oxalato and Azido Groups		
C(1)−C(2)−O(2)	117.1(1)	O(3)−C(1)−O(1)	126.4(1)
C(1)−C(2)−O(4)	116.8(1)	O(4)−C(2)−O(2)	126.1(1)
C(2)−C(1)−O(1)	116.3(1)	N(1)−N(2)−N(3)	177.6(1)
C(2)−C(1)−O(3)	117.3(1)		

Magnetic Results. The molar magnetic susceptibility values (for nickel atom) *vs* *T* of $[\{Ni_2(dpt)_2(\mu\text{-}ox)(\mu\text{-}N_3)\}_n](PF_6)_n$ (2) are plotted in Figure 5. For the two compounds, the χ_M values (4.20×10^{-3} cm^3 mol^{-1} for 1 and 3.63×10^{-3} cm^3 mol^{-1} for 2 at room temperature) increase when the temperature decreases,

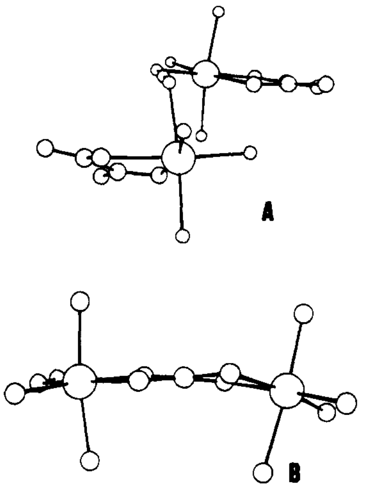

Figure 4. (A) Local coordination of the azido bridge showing the Ni$-N_3-$Ni torsion angle. (B) View of the local coordination of the oxalato bridge along the C$-$C axis, showing the nonplanarity of the Ni$-$ox$-$Ni fragment.

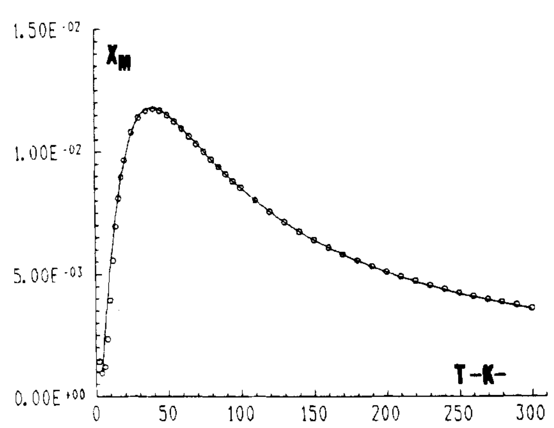

Figure 5. Plot of χ_M versus temperature for $[\{Ni_2(dpt)_2(\mu\text{-ox})(\mu-N_3)\}_n](PF_6)_n$. The solid line corresponds to the best fit calculated as described in the text.

Table 4. Deviation with Respect to the Mean Planes (Å) and Significant Dihedral Angles (deg) for the Two Bridging Fragments Ni(1)$-$Ox$-$Ni(2) and Ni(1)′$-N_3-$Ni(2)

plane 1	O(1)	O(4)	C(1)	C(2)	O(2)	O(3)		
	0.091	−0.087	−0.008	−0.002	0.090	−0.084		
plane 2	Ni(1)	O(1)	O(4)	C(1)	C(2)	Ni(2)	O(2)	O(3)
	0.197	0.000	−0.181	−0.062	−0.058	0.134	0.071	−0.100
plane 3	Ni(1)	O(1)	O(4)	N(4)	N(6)			
	0.078	−0.002	−0.034	−0.035	−0.006			
plane 4	Ni(2)	O(2)	O(3)	N(1)	N(8)			
	0.033	−0.010	0.025	−0.006	0.024			
plane 5	Ni(1)′	N(3)′	N(2)	N(1)				
	0.000	−0.005	−0.006	0.011				
plane 6	Ni(2)	N(1)	N(2)	N(3)′				
	0.000	0.005	−0.010	0.005				

Dihedral Angles between Mean Planes

planes		angle
3	4	22.30
1	3	16.32
1	4	6.52
5	6	102.1

reaching broad maxima at ca. 29 K for 1 and 40 K for 2 with 1.18×10^{-2} cm^3 cm^{-1} value for both compounds. After the maxima the two curves decrease continuously and tend toward zero at low temperatures. According to the structural data provided for compound 2, this system should present two alternating J and J' coupling constants related as $J' = \alpha J$, where α is the alternation parameter. Recently an equation for an alternating system with local spin $S = 1$ has been proposed[13] and the fit of the experimental data with this equation gave the values $J = -26.6$ cm^{-1}, $\alpha J = -13.0$ cm^{-1}, $\alpha = 0.49$, $g = 2.28$, and $R = 9.4 \times 10^{-4}$ for **1** and $J = -27.4$ cm^{-1}, $\alpha J = -2.7$ cm^{-1}, $\alpha = 0.1$, $g = 2.19$, $R = 1.5 \times 10^{-5}$ for **2**, where the quality factor R is defined as $\sum(\chi_M^{calcd} - \chi_M^{obs})^2/\sum(\chi_M^{obs})^2$.

Discussion

Magnetic results indicate that one of the superexchange J parameters found for the two compounds studied in the present work takes a similar value of −26.6 and −27.4 cm^{-1}, whereas the second αJ parameter takes a lower value of −13.0 and −2.7 cm^{-1} for **1** and **2**, respectively. Taking as reference the bibliographic J values for Ni$-$ox$-$Ni and Ni$-N_3-$Ni systems reported to date, assignation of the coupling parameters to our compounds is immediate: for all the nickel$-$oxalato dinuclear systems, in which the nickel atom is placed in a NiN_4O_2 environment, the J parameter has been found[11] in the range −32 to −39 cm^{-1}. This practically constant J value is a consequence of the low flexibility of the oxalato ligand, roughly planar in all cases, which shows no significant differences in the bond parameters in the bridging region.[11] However, the effect of the dihedral angle between the oxalato bridge and the MO_2N_2 planes has been correlated[18] with J for M = Cu(II), for which the J value decreases moderately when the dihedral angle increases. This correlation is also expected for the case M = Ni(II), but to our knowledge, compound **2** is the first example in which the "boat" conformation has been characterized for the Ni$-$Ox$-$Ni system (Table 4). On the basis of this prediction, the J values of −26.6 and −27.4 cm^{-1} for compounds **1** and **2**, respectively, should be attributed to the oxalato bridge superexchange.

In assigning of the αJ value it is interesting to note the structural parameters of the Ni$-N_3-$Ni fragment of compound **2**, for which the Ni$-$N$-$N bond angles are close to 120°, bond lengths are in the 2.127$-$2.209 Å range, and the torsion angle Ni(1)$-N_3-$Ni(2) takes a 102.1° value. In previous papers[7,8] the magnetostructural correlations for azido$-$monobridged nickel systems have been widely studied, and it has been established that the bond angles have a determinant influence on the magnetic properties of this kind of bridge. Here, the azido bridge fragment was modeled as is indicated in drawing **I**, and MO extended-Hückel calculations were performed[19] for the Ni$-N_3-$Ni torsion angle variable, maintaining fixed values for bond lengths and angles, in a similar manner to that reported in our previous papers.[7,8] A modelization in which two xy

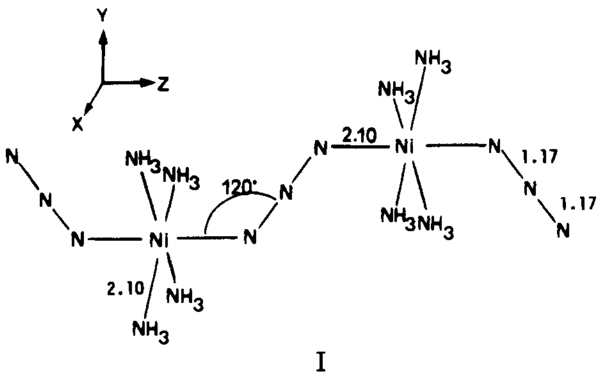

I

---

[18] Alvarez, S.; Julve, M.; Verdaguer, M. *Inorg. Chem.* **1990**, *29*, 4500.

[19] Mealli, C.; Proserpio, D. M. *J. Chem. Educ.* **1990**, *67*, 3399. The CACAO program was kindly supplied by Prof. Mealli.

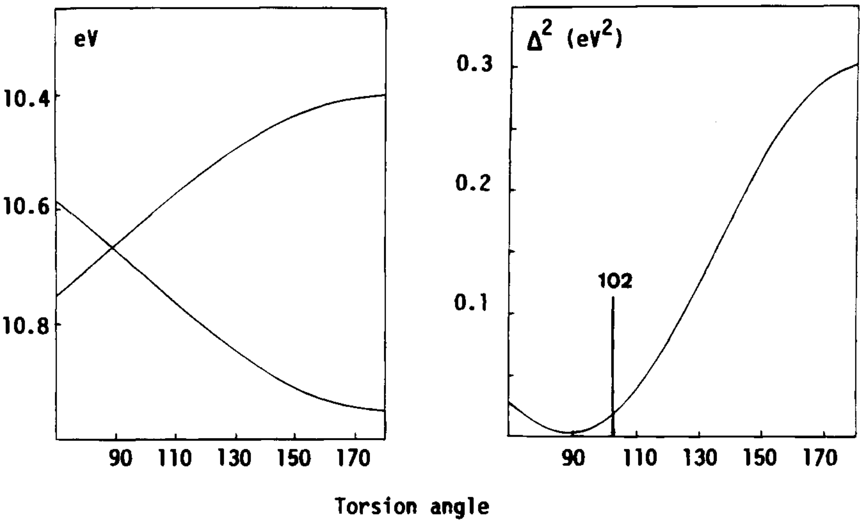

Figure 6. (A) Walsh diagram for the two combinations of the local d_{z^2} magnetic orbitals as a function of the torsion angle Ni–N_3–Ni. (B) Variation of Δ^2 from the above Walsh diagram.

positions of the coordination environment of the nickel atoms are water molecules and the trans position to the bridge is a NH_3 group, is more similar to the real structure of the studied compound ($xy - z^2$ interaction), but the result of the MO calculations is the same, as can be expected from the symmetry of the orbitals. On these basis, we use the same modelization of precedent papers. It is well established that the antiferromagnetic contribution to J is a function[20] of the square of the gaps (Δ) between xy and z^2 pairs of molecular orbitals. For the model employed in these calculations, in which the Ni–N direction is placed along the z axis, the xy orbitals are perpendicular to the chain direction, and the overlap between these atomic orbitals and the bridge is negligible, and consequently, only the square of the gap between the $\Phi z^2_{(s)}$ and the $\Phi z^2_{(a)}$ MOs contributes to the superexchange pathway. In Figure 6 the energy of the $\Phi z^2_{(s,a)}$ MOs and the corresponding Δ^2 in function of the torsion angle is plotted. According to this result, the strongest antiferromagnetic contribution to J should be expected for torsion = 180° and this component decreases when torsion decreases so that it should be zero for a torsion of 90°, which corresponds to an accidentally orthogonal point. It is interesting to point out that this orthogonallity is formally equivalent to the situation obtained for a monoatomic bridge and an Ni–X–Ni angle of 90°, such as is schematized in Figure 7: effectively, for a torsion of 90° one of the nickel atoms overlaps with the π_x MO of the azido bridge whereas the second nickel atom overlaps with the π_y MO of the bridge, in a similar manner to a monoatomic bridge in which the orthogonal orbitals involved in the superexchange are p_x and p_y. From the experimental torsion value of 102.1°, the value of Δ^2 is very low and consequently a small antiferromagnetic contribution should be expected, which results in a final experimental J *value* of -2.7 cm^{-1}, in excellent agreement with the proposed model. This result compares well with the dinuclear compound[21] $(\mu\text{-}N_3)_2[Ni(en)_2]_2(PF_6)_2$, which presents bond parameters close to those of 2 (Ni–N–N bond angles of 121.1° and 119.3° and the Ni–N–N–N–Ni dihedral angle of 68.7°) and a comparable antiferromagnetic magnetic behavior with $J = -4.6$ cm^{-1}.

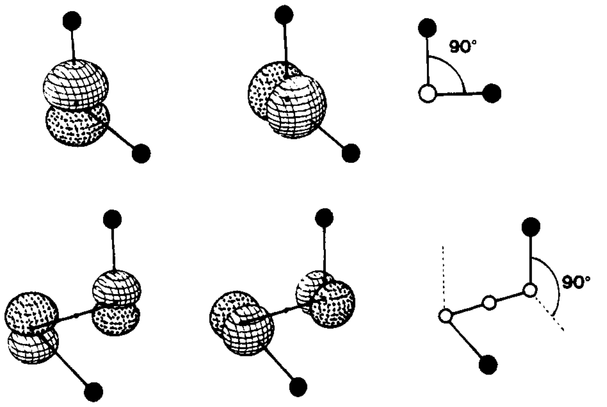

Figure 7. Comparison between the orthogonal p atomic orbitals of a monoatomic bridge and the π MO orbitals of an azido bridge that can overlap with the axial atomic orbitals of the nickel atoms at 90° from the Ni–X–Ni angle or the Ni–N_3–Ni torsion angle.

Concluding Remarks

Structural characterization of an Ni(II) alternating ligand 1D system has been described for compound **2**. From magnetic point of view, compound 2 shows antiferromagnetic behavior with a low alternating parameter $\alpha = 0.1$. The superexchange values $J = -27.4$ cm^{-1} and $\alpha J = -2.7$ cm^{-1} show a remarkable correlation with the N_2Ni–oxalato–NiN_2 fragment in boat conformation and the Ni–N_3–Ni fragment, being the driving argument for the correlation the dihedral angles in the two bridging regions.

Acknowledgment. Financial assistance from CICYT (Grant PB91/0241) is acknowledged.

Supplementary Material Available: Text giving crystal data and details of the structure determination and tables giving atom coordinates, bond lengths, bond angles, anisotropic thermal parameters, and hydrogen atom locations (7 pages). Ordering information is given on any current masthead page.

---

[20] Hay, P. J.; Thibeault, J. C.; Hoffmann, R. *J. Am. Chem. Soc.* **1975**, *97*, 4884.

[21] Ribas, J.; Monfort, M.; Diaz, C.; Bastos, C.; Solans, X. *Inorg. Chem.* **1993**, *32*, 3557.